Synthesis and characterization studies of an organic crystal: 2,6-diaminopyridinium paranitrophenolate paranitrophenol.

Helen Merina Albert[1*], C Alosious Gonsago[2], S Aanadhi[1], G Sundar[2]

[1]Department of Physics, Sathyabama Institute of Science and Technology, Chennai, India

[2]Department of Electronics Science, Mohamed Sathak College of Arts and Science, Chennai, India

Abstract

An organic nonlinear optical single crystal of 2,6-Diaminopyridinium paranitrophenolate paranitrophenol has been grown in the mixed solvent using slow solvent evaporation method at room temperature. For the structural and crystalline analysis, the grown crystal was subjected to single crystal X-ray diffraction, FT-IR and Raman spectral studies. Factor groups were identified and analyzed for the confirmation of IR and Raman active modes of vibrations. Optical absorbance spectrum in the wavelength range 400 to 800 nm has been recorded for the grown crystal which designates the lower cutoff occurs at around 452 nm. Photoluminescence studies were carried out to study the optical emission characteristics. Mechanical behavior of the grown crystal has been studied using Vicker's microhardness tester. The dielectric permittivity, dielectric loss and ac conductivity at room temperature were also investigated using LCR meter. The second harmonic generation efficiency was confirmed by Kurtz-Perry powder test.

Keywords: Crystal growth, XRD, Photoluminescence, Dielectric, Hardness.

Accepted on 28 April, 2021

Introduction

Recently, organic compounds are widely used in the field of laser applications rather than inorganic compounds owing to the ease of tuning the structural properties. Also, organic compounds are also regarded to be excellent futuristic materials for nonlinear optical applications. The structural flexibility of organic compounds is a boon for tailoring the properties of materials suits to our convenience. In the approach of host-guest chemistry, molecule possesses structurally defined hydrogen donor (D)-acceptor (A) motifs which upholds the formation of molecule [1]. The bonding within the framework may vary between strong interactions such as covalent and coordination bonding is relatively weak forces involving hydrogen bonding or interactions. The interactions between the donor and acceptor are assumed to persuade the alignment and thereby set in the nonlinear optical activity.

The co-crystallization of two chromophores (effectively a donor and acceptor) is a common approach for the design of an enhanced second harmonic output. The proton transfer complexes such as dimethyl aminopyridinium 4-nitrophenolate 4-nitrophenol, L-Arginine.

4-nitrophenolate 4-nitrophenol dehydrate have been reported so far. In many crystal lattices of organipplic compounds, the hydrogen bonds are the crucial factor in governing the packing of molecules. Charge-transfer complexes absorb radiation in the visible range, which causes chemical reaction either by addition, condensation and substitution. For Second Harmonic Generation (SHG) to be observed in organic crystals composed of molecules, the crystalline unit cell must lack centre of inversion symmetry. 2,6-diaminopyridine possesses three protonation sites (one lone pair of the tertiary nitrogen atom and two amino groups) and two deprotonation sites (two amino group) [2].

Materials and Methods

AR grade of 2,6-Diaminopyridine (DAP) and aranitrophenol (NP) were recrystallized twice and used as starting reactingmaterials. A molar ratio 1:2 of the above compounds wasrefluxed for nearly 10 hrs using a mixed solvent of toluene andethanol of 75 ml each. One can easily select solvents whichinhibit or promote intermolecular proton transfer. The refluxed solution of 100 ml was prepared at a temperature of with a constant stirring using a motorized magnetic stirrer. The solution was filtered in a clean beaker using filter sheets and then covered with a porous sheet to maintain aconstant evaporation of solvent [3]. The filtered solution was monitored continuously.

A change in colour occurs from light transparent to dark within two days of growth. A long crystal with a flat like morphology appeared in the growth solution after five days. The seed crystal was harvested and placed inside the growth solution and was allowed to grow for a period of 15 days to get an appreciable size of the crystal. 2,6-Diaminopyridine results in noncentric co-crystalline salts with 4-Nitrophenol through hydrogen bonds. The reaction scheme is given below. Chirality in the host-guest complex guarantees the formation of noncentrosymmetric crystal system. Slow evaporation of this solution yields single crystals of 2,6-Diaminopyridinium 4-Nitrophenolate 4-Nitrophenol with an appreciable size as shown in (Figure 1).

***Figure 1**. Single crystals of DAPNP.*

Results and Discussion

The grown crystal DAPNP was subjected to single crystal X-ray diffraction study to analyze the structural characterization. FTIR and Raman spectra were recorded to know the presence of functional groups of the grown compound. Relative SHG output was measured quantitatively by the Kurtz-Perry powder test method. The UV-Visible absorption spectrum was recorded using UV-Vis spectrometer. Photoluminescence spectroscopy technique was used for the electronic and optical characterization. The dielectric behaviour was tested with various frequencies of LCR meter. The microhardness studies were carried out in (020) plane using Vickers microhardness tester [4].

Single crystal XRD

0.1mm3 was used for the analysis. The single crystal X-ray diffraction confirms that the grown crystal belongs to the orthorhombic crystal system. The obtained lattice parameters are in good agreement with the reported values. The crystallographic data are tabulated in (Table 1).

***Table 1.** Lattice parameters of DAPNP.*

Crystal system	**Orthorhombic**
	Pna 21
space group	a=10.866(7) Å, α=90°
Unit cell dimensions	b=12.061(9) Å, β=90°
	c=13.631(8) Å, γ=90°
Volume	1786.41 (8) Å3
Temperature	293(2) K
Wavelength	0.71069Å

Optical studies

The optical absorption spectrum of DAPNP single crystal in the region from 400 to 800 nm is depicted in Figure 2. The presence of absorbance band at around 450 nm indicates that this crystal might be used for second harmonic generation at 1064 nm. However the use of this crystal is limited for optical applications requiring a laser with shorter wavelength, especially shorter than 500 nm. This is mainly due to the presence of paranitrophenol moiety [5]. It is observed that paranitrophenol has a hydroxyl group and a para-substituent of nitro group, the absorption peaks are strongly red shifted. The transition of 4-Nitrophenol is enhanced due to the presence of conjugated groups. When absorption is monitored from low wavelength to high wavelength regions, the lower cutoff occurs at around 460 nm. This may be due to the presence of 2,6-Diaminopyridine and paranitrophenol moieties. This variation in absorption in the UV region can be ascribed to the protonation of the reacting species [6].

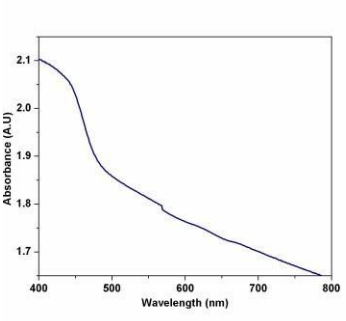

***Figure 2.** Absorption spectrum of DAPNP.*

Photoluminescence studies

Photoluminescence spectroscopy is a commonly used method for characterization of the electronic and optical properties of semiconducting materials and molecules [7]. The recorded Photoluminescence (PL) spectrum of the DAPNP crystal is depicted in (Figure 3).

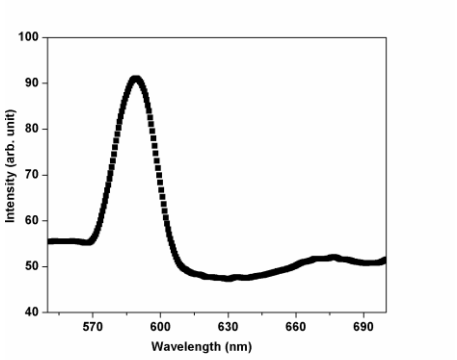

***Figure 3**. PL spectrum of DAPNP.*

The grown DAPNP crystal was excited with a wavelength of 400 nm. The spectrum reveals a broad peak centered at around 585 nm with a low intensity when compared to that of other organic compounds. It is also observed that the intensity gradually decreases in the higher wavelength region. The maximum intensity peak gives rise to yellow emission [8,9]. The proton transfer of aromatic molecules which are hydrogen bonded in the ground state undergoes changes noticeably depending on the kind of substitution on the aromatic ring or functional group.

FT-IR studies

To identify the interaction between 2,6-Diaminopyridine (DAP)and paranitrophenol (NP), FT-IR spectrum was recorded in the range 4000 to 400 cm^{-1} using KBr pellet technique (Figure 4).

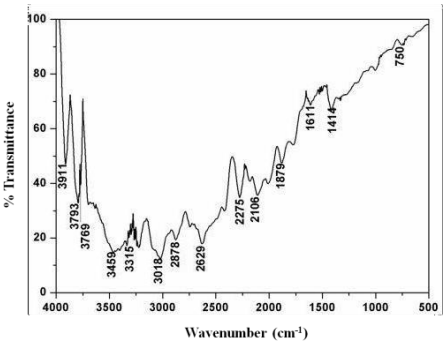

Figure 4*. FT-IR spectrum of DAPNP.*

The band at 3610 cm^{-1} is assigned to the stretching vibrations of O-H group in 4-nitrophenol. The characteristic modes of amino groups in 2,6-diaminopyridine occurred at 3459 and 3315 cm^{-1}. The band at 3018 cm^{-1} is due to the aromatic C-H stretching vibration. The peaks between 2000 and 2300 cm^{-1} are due to combination of asymmetric NH_3 band and its torisional oscillation. The peak at 1611 cm^{-1} is attributed to asymmetric stretching of NH3 + group. The phenolic C-O vibrations yielded a peak close to 1210 cm^{-1} [10].

Raman spectrum

The recorded Raman spectrum of DAPNP in the wavenumber range of 500 to 4000 cm^{-1} is depicted in (Figure 5). A very week at 3073 cm^{-1} may be attributed to aromatic C-H stretching vibrations. The peaks at peaks at 1591 and 1508 cm^{-1} may be due to aromatic ring vibration [11]. The phenolic C-O vibration occurred at 1297 cm^{-1} and 1335 cm^{-1} with the former assignments to the unionized phenolic C-OH and the later to the ionized phenolic C-O (Figures 5 and 6).

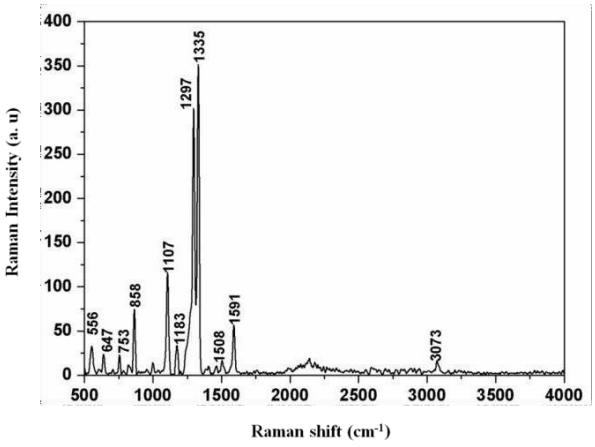

Figure 5. *Raman spectrum of DAPNP.*

Factor group analysis

DAPNP ($C_{17}H_{17}N_5O_6$) crystallizes in orthorhombic Pna21 crystal system with z=4. Application of factor group analysis is to predict the possible vibrational, IR active and Raman active modes. Factor group method developed is applicable to review the vibration behavior of crystals from their symmetry properties [12]. It also provides a basis for the prediction of theoretical IR and Raman spectra of the lattice. A single molecule contains 45 atoms which gives rise to (45>4) 180 atoms in the unit cell. Group theoretical analysis of the fundamental modes of the title complex predicts that there are 540 vibrational modes which include 516 internal modes and 24 external modes such as 9 translational, 12 rotational and 3 acoustical modes. The total possible irreducible modes of vibrations can be divided into four factor group species with decompose into >537=134 A1+135 A2+134 B1+134 B2 and three acoustic modes (A1+B1+B2). The factor group analysis of the title compound was performed by following the procedure outlined byRousseau et al. The summaries of factor group analysis and correlation scheme are presented in (Tables 2 and 3).

Table 2*. Summary of factor group analysis.*

Factor group symmetry	C1 Site symmetry		C	H	N	O	Optical modes	Acoustical modes	Total
C2v	Ext	Int							
A1	3T, 4R	129	51	51	15	18	135	1	134
A2	-	129	51	51	15	18	135	-	135
B1	3T, 4R	129	51	51	15	18	135	1	134
B2	3T, 4R	129	51	51	15	18	135	1	134
Total	9T, 12R	516					540	3	537

Table 3. *Correlation scheme.*

Sl.No	Factor group symmetry	IR Active	Raman Active
537	134A1	-	αxx, αyy, αzz,
	135A2	Z	αxy
	134B1	Y	αxz
	134B2	X	αyz

Here, the polarizability tensors are depicted along the crystallographic X,Y and Z axes. Phonons belonging to A2(Z), B1(Y) and B2(X) are Infrared active are Raman active.

The host guest moieties possess O-H, NO2, C-C, C-O etc. bonds which can be clearly predicted from the experimental measure such as IR. The bonding between the hydrogen atom and the electronegative atom such as N is found to be additional in number. Hydrogen bond network may be

intermolecular or intramolecular in nature due to the presence of pyridinium-phenolate bond.

The bands below 689 cm^{-1} is due to external modes, rotational and translational modes. The translational modes are more intense in IR spectra. Theoretically they are distinguished as 9 translational (3A1+3B1+3B2) and 12 rotational (4A1+4B1+4B2) modes. Experimentally these vibrations can be checked by recording polarized Raman spectra [13].

Dielectric studies

Dielectric studies were carried out in a frequency range of 50 Hz - 2 MHz using LCR meter and further automated using a computer for data recording, storage and analysis. When the grown DAPNP sample was exposed to an applied electric field, the dipole will orient in the direction of the field with the resultant dipole moment. At room temperature, dielectric permittivity and dielectric loss were calculated for different frequencies and are depicted in the dielectric due to permittivity, is polarization of materials and four most important Figure 6 (a) and (b) polarization mechanisms likely electronic polarization αe, ionic polarization αi, orientational polarization αo and space charge polarization. The space charge polarization may take place when mobile charge carriers favour charge migration. The charges get piled up resulting into a localized polarization in the compound. At very low frequencies the dielectric characteristics are influenced by interfacial polarization or at the microscopic level by space charge polarization. The high value of dielectric permittivity at low frequency has been observed which is mainly due to the space charge polarization [14].

The dielectric permittivity (εr) has been computed using the relation

$$\varepsilon_r = \left(\frac{Cd}{A\varepsilon_o}\right) \qquad (1)$$

Where A is the area in square meter, C is the capacitance of the medium in Farad, d is the thickness of the sample in meter and εo is the absolute permittivity in free space having a value of 8.854>10-12 Fm^{-1}. On increasing frequency the hopping transport of localized charge carriers occurs. As it is the charectaristic for ac conduction, in this region 0(n) increases of significantly with frequency, which is demonstrated in the frequency-dependent plot. At the lowest temperatures and/or highest frequencies, this increase is slightly steeper. The frequency independent plateau-like regionobserved in the low frequency region can be attributed to the frequency independent conductivity.

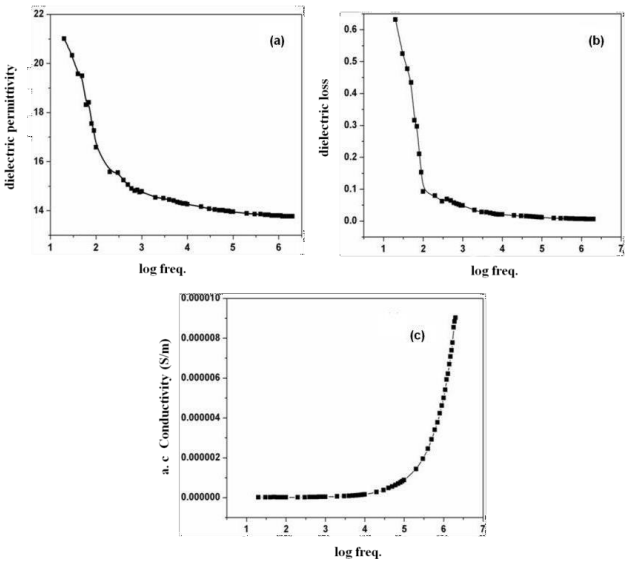

Figure 6*. 6a: Dependence of Dielectric permittivity; 6b: Dielectric loss; 6c: Conductivity with log freq.*

Hardness studies

Mechanical stability is much essential factor for the grown crystal, as far as the fabrication of devices is concerned. Hardness of a material is a measure of the resistance it offers to local deformation. Single crystal of DAPNP was subjected to microhardness measurements using a MATSUZAWA MMTX Vicker's microhardness tester. The observations were carried out at room temperature (Figure 7d) and the indentation time of 5 sec. The hardness of the DAPNP is calculated using the relation.

$$H_v = \frac{1.854P}{d^2}(kg/mm^2) \qquad (2)$$

Where HV is the Vicker's hardness number, P is the indentation load in kg and d is the diagonal length of the impressions in them. To avoid the surface effect, the separation between neighboring indentations was kept more than thrice the diagonal length of indentation impression during hardness measurements. The region of increase or decrease of hardness with the variation in the applied load is called as load dependent hardness region.

The calculation of work hardening coefficient (n) is found using the relation P=adn, where 'a' is the arbitrary constant for a given material, and 'n' is the work hardening coefficient. The plot of log P with log d is a straight line and it is depictedin (Figures 7e and 7f). The work hardening coefficient n is calculated as 1.7, using least-square fitting method. According to Onitsch method, if n>1.6 the material belongs to soft material category and hence the title compound is moderately hard. Hv should increase with P if n>2, decreases with P if n<2. From the hardness value Hv, the yield strength of the material can be found out using the relation.

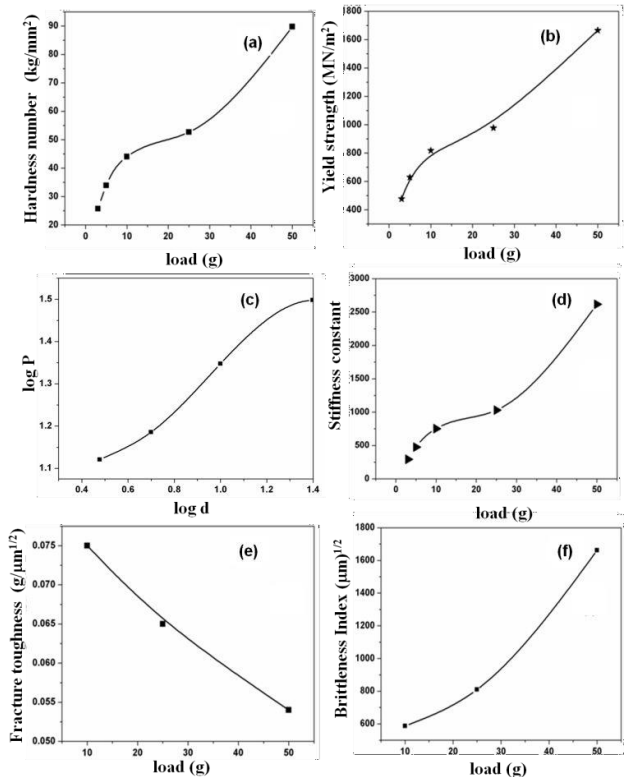

Figure 7. *7a: Load dependence of Hardness number; 7b: Yield strength; 7c: Log P vs log d; 7d: Stiffness constant; 7e: Fracture toughness; 7f: BrittlenessIndex.*

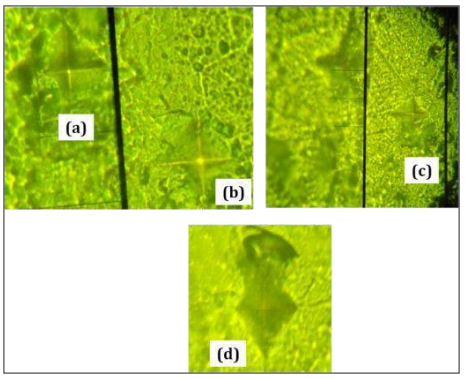

Figure 8. *8a,b,c: Indentation marks on (020) face; 8d: Propagation of crack during indentation.*

For n >2, then

$$\sigma_y = \frac{H_v}{2.9}[1-(n-2)]\left(\frac{12.5(n-2)}{1-(n-2)}\right)^{n-2} \qquad (3)$$

if n<2, then the above equation reduces to

$$\sigma_y = \frac{H_v}{3} \qquad (4)$$

Figure 7a shows the plot of load dependent yield strength. The elastic stiffness constant gives an idea about the nature of bonding between neighboring atoms. This is the property of the material by virtue of which it can absorb maximum energy Before fracture occurs. For various loads the stiffness constant is calculated using Wooster's empirical relation.

$$C_{11}=H_v^{7/4} \qquad (5)$$

The variation of stiffness constant plotted with load is shown in (Figure 7b).

The indentation impressions are associated with the cracks at all loads on (020) planes of the crystal. However, the cracks are well defined beyond a load of 50 g. On increasing the load, hardness number varies, the type of crack that propagates can be determined and the indentation marks are picturized. For which we get median cracks, where c is the crack length 'a' being the length of half-diagonal of the indent. For c/a 2.5, we get palmqvist crack type. For the title compound palmqvist crack has been observed. The fracture toughness (Figure 7c) for the median type of cracks can be measured using the relation (6), where k is 1/7 for the Vicker's indenter, l=c-a for the palmqvist crack type.

$$K_c = kP/(al)^{1/2} \qquad (6)$$

The fracture toughness decreases on increasing the load. The property of brittleness index indicates the intiation of fracture on a test piece determined using the relation.

Table 4 indicates the type of crack observed, variation of hardness number for various loads. (Figure 8) illustrates the indentation marks on (020) face, (d) shows the propagation of crack during indentation.

Table 4. *Hardness behaviour of DAPNP crystal in the (020) face.*

Load P (g)	Hardness number Hv (kg mm-2)	Crack length c (um)	c/a	Nature of crack					
					3	25.7	-	-	-
					5	33.9	-	-	-
					10	44.3	32.78	2	Palm quist
					25	52.65	42.92	1.9	Palm quist

NLO measurement

Second harmonic generation ability of DAPNP was tested by well known Kurtz-Perry powder test. A Q-switched Nd. YAG laser of wavelength 1064 nm with a input of 2 mJ pulse energy with 8ns with a repetition rate of 10Hz was employed. The bulk DAPNP crystal was finely powdered and filled in a microcapillary tube which is exposed to laser radiation. A green emission was observed from the packed sample which indicates the nonlinear optical behaviour and it has been compared with the output of KDP. The SHG output of KDP was 14 mV whereas 19.5 mV was recorded as output for the DAPNP crystal [15].

Conclusion

Single crystals of 2,6-Diaminopyridinium paranitrophenolate paranitrophenol were grown by slow evaporation solution growth technique at room temperature. X-ray diffracton crystallographic studies indicate that the title compound belongs to orthorhombic crystal system. UV–vis studies show the optical response and photo luminescence gives the green emission characteristics of the grown crystal. Factor group analysis enumerates the possible theoretical modes of vibration for the title compound. The hardness study enumerates that the crystal is found to be moderately hard. The stiffness constant, fracture toughness, brittleness index and yield strength of the title material has been evaluated. By employing dielectric studies, the parameters like dielectric loss, dielectric permittivity and ac conductivity has been found. The powder SHG study indicates that the grown 2,6-Diaminopyridinium paranitrophenolate paranitrophenol crystal has nonlinear optical characteristics. With the above results, it may be concluded that the grown single crystal of DAPNP is a potential and suitable material for nonlinear optical applications.

References

1. Ros MB. Organic Materials for Nonlinear Optics NATO Science for Peace and Security Series B. Phys Biophys. 2008;375–90.
2. Gfroerer TH. Photoluminescence in Analysis of Surfaces and Interfaces. Ency Anal Chem. 2006.
3. Stuart BH. Infrared Spectroscopy: Fundamentals and Applications. Anal Tech Sci.2004.
4. Fateley WG, Dollish FR, McDevitt NT, et al. Infrared and Raman Selection Rules for Molecular and Lattice Vibrations.1972.
5. Silverstein R, Kiemle W. Spectrometric Identification of organic Compounds. 2005.
6. Moore N, Carleton B, Blin P, et al. Does ibuprofen worsen COVID-19. Drug Saf. 2020;43:611-14.
7. Kashiwagi E, Shiota M, Yokomizo A, et al. Signaling mediates suppressive effects of celecoxib on androgen receptor expression and cell proliferation in prostate cancer. Prostate Cancer Prostatic Dis. 2014;17:10-17.
8. Franco R, Lillo A, Santisteban RR, et al. Functional complexes of angiotensin converting enzyme 2 and renin angiotensin system receptors: expression in adult but not fetal lung tissue. Int J Mol Sci. 2020;21:9602.
9. Clarke NE, Turner AJ. Angiotensin-Converting Enzyme 2: The First Decade. Int. J. Hypertens. 2012;2012:1–12.
10. Kuhn JH, Li W, Choe H, et al. Angiotensin-converting enzyme 2: A functional receptor for SARS coronavirus. Cell Mol Life Sci. 2004;61:2738–43.
11. Shang J, Ye G, Shi K, et al. Structural basis of receptor recognition by SARS-CoV-2. Nature. 2020;581:221–24.
12. Peiris JS, Lai ST, Poon LLM, et al. Coronavirus as a possible cause of severe acute respiratory syndrome. Lancet. 2003;361:1319–25.
13. Lee N, Hui D, Wu A, et al. A major outbreak of severe acute respiratory syndrome in Hong Kong. N Engl J Med. 2003;348:1986-94.
14. Perlman S, Netland J. Coronaviruses post-SARS: update on replication and pathogenesis. Nat Rev Microbiol. 2009;439–50.
15. Du L, He Y, Zhou Y, et al. The spike protein of SARS-CoV a target for vaccine and therapeutic development. Nat Rev Microbiol. 2009;7:226–36.

*Correspondence to

Dr. Helen Merina Albert

Department of Physics

Sathyabama Institute of Science and Technology

Chennai

India

E-mail: merinagonsago@gmail.com